HHS Public Access

Author manuscript

Biomaterials. Author manuscript; available in PMC 2020 May 26.

Published in final edited form as:

Biomaterials. 2019 February ; 192: 226–234. doi:10.1016/j.biomaterials.2018.11.005.

Active wrinkles to drive self-cleaning: A strategy for anti-thrombotic surfaces for vascular grafts

Luka Pocivavsek[e,*], **Sang-Ho Ye**[a,d], **Joseph Pugar**[b], **Edith Tzeng**[a], **Enrique Cerda**[c], **Sachin Velankar**[b,f,**], **William R. Wagner**[a,b,d]

[a]Department of Surgery, University of Pittsburgh Medical Center, Pittsburgh, PA, 15213, USA

[b]Department of Chemical Engineering, University of Pittsburgh, Pittsburgh, PA, 15213, USA

[c]Department of Physics, Universidad de Santiago de Chile, Santiago, Chile

[d]McGowan Institute for Regenerative Medicine, University of Pittsburgh, Pittsburgh, PA 15219, USA

[e]Department of Surgery, The University of Chicago, Chicago, IL, 60637, USA

[f]Department of Mechanical Engineering, University of Pittsburgh, Pittsburgh, PA, 15213, USA

Abstract

The inner surfaces of arteries and veins are naturally anti-thrombogenic, whereas synthetic materials placed in blood contact commonly experience thrombotic deposition that can lead to device failure or clinical complications. Presented here is a bioinspired strategy for self-cleaning anti-thrombotic surfaces using actuating surface topography. As a first test, wrinkled polydimethylsiloxane planar surfaces are constructed that can repeatedly transition between smooth and wrinkled states. When placed in contact with blood, these surfaces display markedly less platelet deposition than control samples. Second, for the specific application of prosthetic vascular grafts, the potential of using pulse pressure, i.e. the continual variation of blood pressure between systole and diastole, to drive topographic actuation was investigated. Soft cylindrical tubes with a luminal surface that transitioned between smooth and wrinkled states were constructed. Upon exposure to blood under continual pressure pulsation, these cylindrical tubes also showed reduced platelet deposition versus control samples under the same fluctuating pressure conditions. In both planar and cylindrical cases, significant reductions in thrombotic deposition were observed, even when the wrinkles had wavelengths of several tens of μm, far larger than individual platelets. We speculate that the observed thrombo-resistance behavior is attributable to a biofilm delamination process in which the bending energy within the biofilm overcomes interfacial adhesion. This novel strategy to reduce thrombotic deposition may be

[*]Corresponding author. Luka.Pocivavsek@uchospitals.edu. [**]Corresponding author. Department of Chemical Engineering, University of Pittsburgh, Pittsburgh, PA, 15213, USA. velankar@pitt.edu (S. Velankar).

Data availability

All experimental data required to reproduce the findings from this study will be made available upon request.

Conflicts of interest

Since the conclusion of this research, our research team is seeking to commercialize this technology.

Appendix A. Supplementary data

Supplementary data to this article can be found online at https://doi.org/10.1016/j.biomaterials.2018.11.005.

applicable to several types of medical devices placed into the circulatory system, particularly vascular grafts.

Keywords

Dynamic topography; Biofouling; Platelet deposition; Thrombosis; Active surfaces; Pulsatile flow

1. Introduction

The inner lining of arteries excel at resisting unwanted fouling, most importantly avoiding thrombotic deposition. This anti-fouling ability is attributable to a broad variety of passive and active mechanisms employed by the endothelial cells that line the internal surfaces of the entire circulatory system [1]. In comparison, synthetic surfaces are less adept at resisting thrombotic deposition, and the use of such surfaces is limited to certain devices and often must be accompanied by the provision of anticoagulant and anti-platelet therapy. There has been an enormous effort in the medical community over the past several decades to create synthetic surfaces that resist fouling for use in catheters, dialysis devices, and vascular implants such as heart valves, and prosthetic blood vessels [2]. The various strategies that have been employed for improving hemocompatibility include fluorination of surfaces [3], bonding heparin to the surface [4], and modification with polyethylene glycol or phosphorylcholine and similar zwitterionic groups [5–7]. Some of the resulting surfaces can be used for long term blood contact, e.g. for heart valves or vascular grafts. Nevertheless, for vascular conduits, clinical studies have shown that such surface modifications have had limited long-term benefit in improving graft patency [8–10]. On the whole, synthetic grafts, typically made of polytetrafluroethylene (PTFE) or polyester, perform poorly in bypasses to blood vessels below the knee. In such surgeries, autologous (i.e. the patient's own) veins have higher rates of patency, and hence are the preferred conduit. The down side of these vein conduits is the morbidity associated with the additional surgery needed to harvest the vein.

The majority of the approaches mentioned above for improving synthetic surface hemocompatibility are chemical in nature and involve the modification of the chemical composition of the blood contact surface, e.g. fluorination reduces surface adhesion strength [3], polyethylene glycol provides a highly hydrated surface [11], and heparin bonding provides anticoagulating and antiplatelet effects [12]. In this article we examine a very different approach: antifouling activity of surfaces induced by topographic changes of the blood-contacting surface.

Many surfaces in nature are endowed with non-flat surface morphology or topography [13,14], and many of these (e.g. surfaces of lotus leaves, rose petals, mussel byssus, sharkskin, and gecko feet) have attracted intense attention in the technological community due to their role in tuning wettability, friction, and adhesion [15]. Many conduits in the body (arteries, esophagus, trachea, small intestine) are heavily corrugated or wrinkled. Arteries, in particular, exhibit wrinkles that can fully or partially flatten out as the arteries dilate or distend in response to blood pressure changes during the cardiac cycle [16,17]. Because

structure in biology typically serves a function, we hypothesize in Pocivavsek et al. [18] that this cyclical fluctuation in luminal topography in arteries confers an anti-thrombotic function.

In fact, past research has explored the antifouling surface activity due to non-flat topography, or surface deformation, or both. For instance, recent reviews have cited numerous examples of static topographies that reduce marine [19] or bacterial [20] biofouling and the corresponding technology has been commercialized under the name Sharklet. Several articles have also examined the effect of static surface topography on blood biofouling [21–26]. Turning to surface deformation, Shivapooja et al. examined marine fouling on elastomeric surfaces and showed that simply stretching the elastomer would release the foulant [27,28]. More complex surface deformations, e.g. by embedding pneumatically-inflatable bubbles under the elastomeric surface, was shown to be even more effective, and the same approach was used to develop a multi-lumen urinary catheter which could be pneumatically-actuated to remain clean [29]. More recently, Gu et al. [30] examined biofilms that formed on topographically-patterned shape-memory polymer surfaces. Mild heating induced shrinkage of the polymer and detachment of the biofilm.

We now turn to dynamic topography, i.e. an active surface whose topography changes repeatedly. In Pocivavsek et al. [18], we proposed a new mechanism in which actuation from a smooth to a wrinkled surface induces delamination of a film adhered to the surface. In that article, the topography was characterized by a wavelength λ and amplitude A, which corresponds to a characteristic surface curvature $\kappa = A/\lambda^2$. As the surface transitions from smooth to wrinkled, A increases, and hence κ increases in tandem. We showed that if a soft elastic film is adhered to such a surface, at some critical amplitude A_c, or equivalently, critical curvature $\kappa_c = A/\lambda_c^2$, the adhered film patch begins to delaminate from the wrinkled surface. The mechanism underlying such delamination will be discussed further in Section 3.

In this report, we test whether this concept of deadhesion driven dynamic topography, i.e. repeated cyclical wrinkling and unwrinkling, can be an effective anti-fouling mechanism for surfaces in contact with blood. More specifically, we seek to lay the ground for new kinds of vascular grafts that rely on continuous topographic actuation to stay clean.

2. Experimental results

The experimental section of this paper is organized to clearly emphasize the distinction between two different experimental platforms. The first was developed to provide initial proof of principle of the central hypothesis that topographic actuation reduces the deposition of platelets from whole blood. The second represents a step towards clinical translation. Both platforms are pneumatically actuated, but in the first (Section2.1) the pneumatic actuation (using water) is only a means of stretching an elastomeric surface, analogous to stretching the surface of a balloon by inflation. In principle, the same results as Section 2.1 may be obtained by stretching the surface by any other method. In the second approach (Section 2.2), cylindrical tubes are fabricated which are inflated and deflated by pressurizing

the blood itself. This is analogous to the diameter changes of arteries under pulse pressure [31].

2.1. Wrinkling on planar surfaces

As a first test, we considered surfaces that were approximately planar, but capable of transitioning from being wrinkled to being smooth when stretched. The essential mechanics of the experiment are illustrated in Fig. 1A–D. An elastomeric sheet endowed with a wrinkled surface (see next paragraph) was bonded to a pneumatic actuator base that could be pressurized, causing the sheet to balloon outwards. The stretching of the sheet then smoothed out the wrinkles. With repeated pressurization and depressurization cycles, the surface could be transitioned continually between wrinkled and smooth textures. The wrinkled surface was itself generated using UV-ozone (UVO) treatment of polydimethylsiloxane (PDMS) silicone rubber. The mechanical platform is similar to that used by Shivapooja et al. [27,28], with the central difference being that inflation is used to drive a wrinkle-smooth transition at the surface.

Most of the experimental details are given in the ESI, but briefly, an pneumatic actuator base (Fig. 1E) cast from silicone RTV-4136 M (Dow Corning) was constructed (Fig. 1E) and a 5 mm thick sheet of Sylgard 184 PDMS rubber was bonded to it (Fig. 1F,G,I). The exposed surface of the Sylgard elastomer sheet was then subjected to ultraviolet-ozone (UVO) treatment, which is known to vitrify the surface into a ~100 nm thin layer of silica which is much stiffer than the elastomer [32].

Some samples were UVO-irradiated with the elastomer film being flat (i.e. the actuator base was not pressurized during ozonolysis). These samples served as controls. Wrinkled samples were generated by irradiating under pressurized conditions when the elastomeric film was distended, i.e the state of Fig. 1G. Due to the rectangular geometry of the ballooning sheet, the elastomer stretching is predominantly uniaxial, and experiments used a stretching of 30% along the short axis. The silica layer formed due to UVO treatment was strain free under pressurized conditions, but upon reducing the pressure, the elastomer retracted and compressed the silica layer, leading to wrinkling of that layer with a uniform wavelength of roughly 50 μm (Fig. 1I). Given the anisotropic strain along the actuator short axis, the neutral direction of the wrinkles was along the actuator long axis.

Platelet deposition experiments used two actuator chambers working “in opposition” so that one chamber inflated while the other deflated (Fig. 2A). The blood contact device comprised a polycarbonate frame sandwiched between two elastomeric sheets prepared as per the previous paragraph (Fig. 2B). Valves on the polycarbonate frame allow easy filing of the reaction chamber with blood (green water is used in Fig. 2B for illustration) and purging of all air. Once the chamber was filled with 30 mL of fresh ovine blood [7] (See ESI), the actuator bases were connected to a peristaltic pump (Fig. 2C). During each half-cycle, the pump moved 4 mL of water from one actuator base to the other. This pressurized one actuator base inflating its elastomeric sheet to a smooth state while depressurizing the other and contracting its elastomeric sheet to a wrinkled state. The entire chamber was place in a tissue culture incubator at 37 ℃ and actuated at 0.4 Hz/cycle for 90 min or 2100 cycles. This experimental setup offers several advantages: it minimizes contact of blood with non-target

surfaces; air is completely excluded; the blood itself is never placed in the flow circuit and hence does not experience high-shear flow; the counter-pulsation minimizes hydrostatic pressure buildup in the blood-containing chamber; and two samples can be tested simultaneously.

For the static PDMS control samples, the surface thrombotic deposition was assessed by placing the samples in ovine blood and gently rocking for 90 min at 37 ℃ on a hematology mixer (see ESI).

At the end of blood contact, the surfaces were washed with saline and cut into 1 cm^2 samples taking care to exclude regions near the ends of the inflation zone where substantial bi-axial strain exists. Samples then underwent post-processing for lactate dehydrogenase (LDH) and scanning electron microscopy (SEM) characterization [33,34].

The results of this experiment are shown in Fig. 3. The PDMS surface that had been UVO-treated without prestretching (and hence remained smooth), exhibited significant thrombus formation after exposure to blood under static conditions (Fig. 3A). The PDMS surface that had been UVO-treated with prestretching (and hence wrinkled), demonstrated even greater thrombus formation when exposed to blood under static conditions (Fig. 3B and E). When exposed to blood under continual actuation, both smooth and wrinkled surfaces showed dramatically lower platelet deposition: 84% lower in the case of smooth surface actuation (Fig. 3C and E) and 97% lower with wrinkled-surface actuation (Fig. 3D and E). The effect of the surface topography is more evident in Fig. 3F which compares the smooth vs wrinkled surfaces under actuation. The topographically-actuated wrinkled surfaces were nearly completely devoid of deposited platelets and showed the platelet deposition to be 73% lower than the actuated flat systems. These findings indicate that repeated stretching – by itself – reduces platelet deposition of interface surfaces. The continually actuating surface topography further reduces thrombus formation by several fold.

2.2. Tubular constructs: wrinkle actuation by pulsatile pressure

Fig. 3 supports the basic hypothesis that a surface that continually transitions between a smooth and wrinkled state has anti-fouling activity against blood. If cylindrical tubes can be endowed with such actuating topography on their inner surface, they may be useful as vascular grafts. The immediate question that arises is: how can such surfaces be continually actuated when they are implanted into the human body? We propose that the pulsatile flow of the cardiovascular system can itself be used as a freely-available driving force for continuous actuation. Specifically, natural arteries are known to expand and contract several percent with every pulse cycle [31]. These blood pressure pulsations may be harnessed to drive small amplitude stretching and relaxation of the synthetic grafts, which can then induce continual changes between smooth to wrinkled states at the luminal surface. The concept is illustrated in the bottom two images of Fig. 4B where a cylindrical tube endowed with a stiff inner wall is wrinkled in a low pressure state, but smooth when inflated to a higher pressure state.

The goal of this section is to take a first step towards this concept. We fabricate cylindrical tubes and test their fouling under blood exposure under continual pulsation. Secondarily, we also examine the effect of wavelength on the antithrombotic activity.

The materials selected for the cylindrical constructs were entirely two-part silicone elastomers. The luminal film was made from Xiameter RTV-4136 M, whereas the thick portion of the tube wall was composed of a much softer material, GI-245 (Silicones, Inc.). Tensile testing (See ESI) shows that the modulus of the RTV-4136 M and GI-245 is 2.6 MPa and 0.029 MPa respectively. It is this large modulus mismatch that induces luminal wrinkles when the luminal film experiences compressive stress.

The fabrication method for constructing such tubes is illustrated in Fig. 4A. The fabrication details are given in the ESI, but briefly, a several-micron thick film of the silicone RTV-4136 M was spread onto a flat acrylic surface and cured. A thick layer of the softer silicone (GI-245) was then spread on this first layer and allowed to cure to form a bilayer. Upon releasing from the acrylic surface, this bilayer is stress-free and therefore remains flat and has a smooth surface. In order to create surface wrinkles, this bilayer was then bonded to a second layer of GI-245 (which had been cast separately) which was held prestretched 30–40%. Upon releasing the prestretch, the stiff surface film of RTV-4136 M developed strong wrinkles whose wavelength could be tuned by varying the film thickness. The layered sheet was then rolled into a cylinder 10 cm long and 6 mm in diameter (wrinkle-side inside) and the edges of the cylinder were sutured together. The suture line was sealed externally with a thin coat of GI-245 silicone to provide a water tight suture line. Finally, a layer of a different silicone, GI-380, was used to so that the tubes would give the desired expansion/contraction at physiological pressures. We emphasize that the luminal film of all samples was cast against optical quality acrylic sheets, and hence all samples are expected to have the same nanoscale roughness. Thus, while nanoscale roughness is known to affect platelet deposition [35–37], this fabrication technique ensures consistency across all samples. The selection of geometric parameters (e.g. thicknesses of the various layers, the degree of prestretch, etc.) was optimized empirically. Typically, with pre-stretch of less than 10%, wrinkles developed inconsistently and weakly, whereas strains exceeding 20% gave reliable wrinkles that were uniform over the entire surface. With an eye towards future experiments, the grafts were designed so that the two pressures would be close to typical diastolic and systolic pressures (Fig. 4B). It must be noted that the compressive strain that induces wrinkling comes from both the prestretch as well as the strain associated with bending a flat sheet into a cylinder shape. An image of the resulting cylindrical tube sliced length-wise as well is shown in Fig. 4C.

Before conducting blood flow experiments, it is critical to identify the pressure at which wrinkles appear and disappear. Since the resulting tubes are opaque, this validation cannot be done by simple visualization or microscopy. To perform this validation, we used Optical Coherence Tomography (OCT) using a specialized catheter [38]. OCT works by collecting images along circumferential cross-sections at high frequencies and has been used to examine the luminal and mural structure of arteries *in vivo*. With current OCT technology, the lateral spatial resolution is approximately 50–100 μm. For the validation, the silicone graft was sealed at one end, and the other end was connected to a syringe pump. The graft

was inflated and deflated at 0.05–0.1 Hz with water while measuring pressure. Simultaneously an OCT catheter was swept through the graft to image the lumen. Fig. 4D shows the OCT images measured during this calibration along with the measured pressures. It is clear that the lumen becomes much less wrinkled as the pressure is raised from 50 mm Hg to 200 mm Hg. These pressures, which are in the range of diastolic and systolic pressures in humans, provide the desired pressure range for the following blood fouling experiments.

After calibration of each graft, blood tests were conducted using fresh whole blood from a healthy human donor (see details in ESI). Static (i.e. unactuated) control samples were tested in a rocking configuration similar to those in the previous section so that the blood was constantly shaken gently. The actuated samples were tested as follows. Multiple cylinders with three different wavelengths (1000 μm, 250 μm, and 80 μm) were tested. A vascular access catheter was sutured at one end of the graft, whereas the other end was sutured closed. The catheter access line was split to allow a syringe pump and blood pressure analyzer to be connected simultaneously. The entire system was incubated at 37 ℃ and actuated for 90 min. The actuation volume was set so that the desired high and low pressures, identified from the OCT calibration experiments, were reached. At the end of the blood exposure, the cylinders were cut open and analyzed with an LDH assay (see ESI for details).

The results are shown in Fig. 5. Fig. 5A compares the cross-sections under fully-deflated conditions of the four grafts used in blood tests: one graft with a smooth lumen, and three with wrinkles of various wave-lengths. The native silicone graft was thrombotic under static conditions. As a comparison, a $TiAl_6V_4$ surface was also exposed to blood under static conditions, and it showed only slightly lower platelet deposition. For the grafts undergoing continual actuation between expanded (smooth) and contracted (wrinkled) states, the sample with a 1000 μm wavelength showed 70% lower platelet adhesion than the control samples. The grafts with smaller wavelengths showed an even sharper decrease in platelet adhesion, with the smallest wavelength exhibiting 88% lower platelet deposition than the static control.

In fact, the difference between the samples is even larger than apparent from Fig. 5B because of the significant platelet adhesion evident along the suture line. It is well known that suture lines are a strong nidus for platelet activation/adhesion and thrombus formation. We therefore also reanalyzed the data for the sutured samples examining only the sutureless hemicylinder, (Fig. 5C). Excluding the effect of sutures, the actuated graft with the smallest wavelength had 50-fold lower fouling than the static control, and 5-fold lower fouling than the actuated graft with the largest wavelength.

Similar experiments were also conducted using grafts with a completely smooth lumen, and these results were similar to the lumen with 1000 μm wavelength. This suggests that the 1000μm wavelengths under actuation is, from a blood biofouling perspective, equivalent to a flat surface under actuation.

3. Discussion

To summarize the main results, we show that surface actuation between wrinkled and flat surfaces reduces platelet deposition, and moreover dynamic topography is more effective at avoiding platelet fouling as its wavelength reduces. It is noteworthy that the surface chemistry of the cylindrical constructs (bare silicone) is altogether different from the flat sheets used in the previous section (silica-like surface bonded to silicone). This suggests that the effect noted is due to topographic actuation and is not specific to the surface chemistry. Due to the difficulty of observing the surface while under constant actuation, we have not yet attempted to elucidate the mechanics by which topographic actuation resists blood fouling. In this section, we will first propose two possible mechanisms, one based on adhesion and a second based on flow/kinetic effects.

The adhesion-based explanation is that for a solid-like foulant to adhere onto a curved surface, it must either deform or have a reduced contact with the surface. This either poses an elastic energy penalty (if the foulant deforms along with the surface) or reduced adhesion strength (if the foulant does not deform), either of which could reduce fouling. Yet the results above show that fouling reduces considerably even at wrinkle wavelengths that are at least an order of magnitude larger than the size of platelets. Thus, such an adhesion-strength-based explanation, if applicable, cannot operate on the level of single platelets. Yet platelets are generally not present on a surface singly, but instead in the form of a collection of platelets, i.e. a thrombus. In thrombus formation, platelets from blood adhere to a surface and begin to aggregate into patch-like structures [39], which can be several tens of microns in size. The adhesion-based mechanism can then be summarized in cartoon form (Fig. 6). It illustrates a patch of thrombus that is large enough that it begins to behave as an elastic continuum and therefore responds to the changes in topography of the substrate. As the surface wrinkles, the patch seeks to deform conformally, but the change in curvature imposes an elastic energy penalty. Beyond a certain curvature, the increase in elastic energy forces delamination.

It is precisely this physical picture of Fig. 6, dubbed “topography-driven delamination”, that has been developed quantitatively in Pocivavsek et al. [18] Briefly, we considered a flat substrate to which is adhered a soft elastic layer. As in the research conducted here, the flat substrate itself comprises a thin stiff surface film (thin blue line in Fig. 6) that is bonded to a softer underlayer (orange layer in Fig. 6). Therefore compressive strain induces the substrate to transform from flat to an approximately sinusoidal texture (wavelength λ, amplitude A). Due to the mechanics of buckling of a stiff film bonded to a soft underlayer [40], neither the area nor the wavelength change significantly during the buckling process; the main effect of the compressive strain is to increase the amplitude. Once the amplitude reaches a critical value, the adhering layer starts to delaminate. We showed that physics of such delamination can be captured by two parameters. The first parameter is the curvature $k \propto A/\lambda^2$ which quantifies the changes in topography. The second parameter is the elastocapillary lengthscale, ℓ_{ec}, which depends only on the properties of the adhering layer (mod-ulus, thickness, adhesion strength). We showed that the criterion for deadhesion is $k\ell_{ec} > 1$, or equivalently, that the adhering layer delaminates when the curvature exceeds a critical value

$k_c = 1/\ell_{ec}$. More flexible patches have smaller ℓ_{ec} values, and hence need a larger curvature, i.e. larger amplitude, to deadhere. As clarified in Pocivavsek et al. [18], this newly proposed mechanism of topography-driven de-lamination is altogether different from the other well-known mechanisms of delamination [41]. More specifically, a detailed comparison [18] between edge delamination, buckle delamination, and topography-driven delamination shows that surface topography is more effective at increasing the energy release rate that drives delamination of the adhered layer.

The experiments (Fig. 5C) unambiguously show that platelet deposition reduces (i.e. anti-thrombotic activity improves) as wavelength decreases. This observation is entirely consistent with this newly-proposed mechanism of topography-driven delamination [18]. To illustrate this, let us treat the aggregation of platelets into surface-adhering thrombus patches as a random process such that the surface is covered with patches having different structures, geometries, and mechanical properties. All this variability in thrombus properties may be captured as a statistical distribution $P(\ell_{ec})$ of the elastocapillary length, where more flexible patches correspond to smaller values of ℓ_{ec}. The surface transitions from an initial flat topography (initial curvature $\kappa_i = 0$) to some final wrinkled topography (the final curvature, $k_f \propto A/\lambda^2$). Since the topographic change preserves interfacial area, given a certain strain driving the topographic changes, $A \propto \lambda$, and hence $k_f \propto 1/\lambda$. Thus, according to the deadhesion criterion above, patches with $k_f \ell_{ec} < 1$ will deadhere, whereas relatively flexible patches will $(k_f \ell_{ec} < 1)$ remain adhered. Since $k_f \propto 1/\lambda$, the fraction of adhering patches will reduce as wavelength reduces, as indeed seen experimentally.

This argument may be made more quantitative by selecting a specific form for the distribution function $P(\ell_{ec})$ In the ESI we show that a simple exponential form for $P(\ell_{ec})$ predicts that the number of adsorbed platelets should be proportional to the wavelength λ. Thus for the three experimental wavelengths of Fig. 5C and 1000 μm, 250 μm and 80 μm, this simple statistical model suggests that the platelet ad-sorption should be in the ratio 1:0.25:0.08. The experimentally-observed ratios (1:0.51:0.2, from Fig. 5C) show a similar trend but are weaker than predicted. Nevertheless, the central point of this statistical model is that the mechanism of topographically-driven delamination predicts a quantitative relationship between foulant adhesion and wavelength such that decreasing wavelength also decreases adhesion.

A second potential explanation is based on the kinetics of platelet attachment. All of the samples evaluated in this study, even the static ones exposed to rocking contact with blood, experience some blood flow. We acknowledge that this blood flow is not necessarily representative of what would be encountered *in vivo*, nevertheless, the syringe pumps used to drive the reciprocating flow provide good mixing conditions to ensure that any platelets that become activated remain distributed homogeneously throughout the fluid, and can get trans-ported by flow and diffusion everywhere on the test surface. It is well-known that platelets can spread upon attaching to a surface over a timescale of several seconds or minutes [42]. We speculate that in our case, since the surface is constantly evolving over a timescale faster than the spreading kinetics, the corresponding near-surface flow may

continually remove the platelets before they can attach firmly. In a more phenomenological sense, clinicians generally identify stasis (i.e. lack of blood flow) as a prime contributor to thrombosis. For instance, the higher likelihood of thrombosis near an arterial bifurcation is often associated with thrombosis because the stagnant flow allows sufficient time for deposition. If topographic actuation improves radial mixing between the slow-moving blood near the surface and the faster-moving bulk, individual platelets would not persist near the surface long enough to spread, and hence the platelet deposition may be reduced. Yet, while such flow/kinetics effects may contribute to the anti-thrombotic activity in our experiments, it does not readily explain the observed wavelength-dependence of the antithrombotic activity. In fact one would expect longer wavelengths to disrupt the near-surface fluid layer over longer distances, and therefore decrease platelet adhesion to a greater extent – the opposite trend to what is observed. In contrast, the wavelength dependence that is actually observed in experiment arises naturally from the adhesion-based mechanism of topography-driven delamination.

We will now place our results in the context of past research which seeks to use mechanical deformation for antifouling. Lopez et al. have previously reported that stretching of an elastomeric surface can induce deadhesion of a foulant layer [27–29]. However, this phenomenon has, to our knowledge, never been demonstrated for blood fouling. The significant decrease in platelet deposition due to diameter pulsation of the grafts observed in our experiments is consistent with these past observations. The issue of topographic actuation has also been examined previously to some extent. Shivapooja et al. showed that voltage-induced topographic deformation of dielectric elastomers could induce detachment of bacterial biofilms attached to the surface [27]. Gu et al. reported that a macroscopic shape change of polymer sheet would drive a roughly affine shape change of a hexagonal pattern imprinted on that sheet [30]. This would also drive detachment of a bacterial biofilm. In both these cases, the surface undergoes in-plane strains; globally in Gu et al. [30] (since the shape memory polymer undergoes macroscopic deformation), and local in Shivapooja [27] (most of the surface expands whereas some regions contract). In contrast, the topographic actuation examined here is – to a first approximation – a purely bending deformation with no changes in area. Due to the large mismatch in elastic modulus between the silica surface layer and the silicone (Section 2.1) or between the two silicones (Section 2.2), the surface itself accommodates stretching by simply straightening out. In this regard, the microscale mechanics of antifouling action in this report most resembles the work of Epstein et al. who also used UVO-treated PDMS surfaces to examine whether wrinkles would reduce bacterial biofouling [43]. Their results were ambiguous: only with wavelengths of roughly 1 μm did they note a decrease in biofouling with the topographic actuation. Sub-micron or 2 μm wavelengths gave inconsistent results. In contrast, we detect strong anti-fouling activity towards blood at wavelengths that are over an order of magnitude higher.

Finally, we note the technological implications of this research. The first, most obvious one is that continual topographic transition of a surface between highly wrinkled and less wrinkled states has an anti-thrombotic effect. Second is the method of driving the topographic transition. Any dynamic surface must have some driving force to actuate the surface. This may be pH for materials based on hydrogels, temperature for shape-memory metals or shape-memory polymers, mechanical pressure for pneumatic actuation, or light for

liquid crystal elastomers. Yet for medical applications, complex actuation mechanisms and the need to power them pose significant hurdles. However, in the cardiovascular system, we can harness the natural cardiac cycle and pulse pressure to drive topographic changes in vascular grafts. This may allow practical implementation of topographic actuation in vascular grafts without the need for external power sources. The grafts discussed in Section 3.2 of this paper are not designed for this: while the pressure needed for topographic actuation is within the range of physiological pressure, the corresponding diameter changes are too large for practical implementation. Moreover the industrial silicone materials are not suitable for implantation. Nevertheless, with suitable selection of compliant materials and controlling the prestrain during the fabrication, topographic actuation using pulse pressure variations may be possible. The practical viability of such approaches can only be judged after *in vivo* animal implantation studies that are beyond the scope of this paper. These *in vivo* animal experiments would also address the effect of dynamic topography on the adhesion of other constituents of blood such as leukocytes or proteins. Our present *in vitro* studies did not assess these other constituents directly, although we note that leukocyte deposition was not seen on any of our samples exposed to whole blood. Third, we emphasize that – even though the mechanism of anti-thrombotic action is not entirely clear – the effects seem to be in-dependent of surface chemistry. Accordingly these purely "mechanical" effects may be used synergistically with any chemical modification of the surface. Fourth, since nothing about the employed materials or surfaces was optimized for blood contact, the mechanism of anti-fouling action inducted by topographic manipulations may be general and therefore useful for other kinds of fouling, e.g. bacterial biofouling or mineral deposition. Finally we note that topographic surface patterns can also be tailored to encourage adhesion and proliferation of cells, selective growth of certain cell types, or migration of cells [44–47]. This general approach is called contact guidance [48,49]. Thus, delamination driven by dynamic topography may be used in conjunction with contact guidance for precise control of species that do and do not ad-here to a surface.

4. Conclusion

In summary, the central results of this paper are as follows. (1) A surface that continually expands and contracts is able to resist platelet deposition compared to the same surface held static. (2) A further de-crease in platelet deposition can be realized if the surface undergoes cyclical topographic changes from being highly wrinkled to being much less wrinkled or smooth. (3) The deposition resistance is improved by topographies with smaller wavelengths, at least within the range of wavelengths examined. (4) Finally, progress towards a practical implementation of this system for vascular grafts is reported where the pulsatile pressure of the circulatory system may itself be used to drive the topological actuation.

Finally we note that while the focus in this paper was on vascular grafts, the principle anti-fouling using topographically-actuating surfaces may be applicable more broadly, both in the context of other blood-contact application, as well as non-medical applications.

Supplementary Material

Refer to Web version on PubMed Central for supplementary material.

Acknowledgements

We thank Pitt Undergrad Engineering team for help with initial actuator fabrication and design. We thank Dan McKeel for help with machining of bioreactor parts, Dr. Toma Catalin and Dr. Francois Yu for help with OCT setup, and Nicholas R. Moriarty and Julie Hecht for assistance in image processing. We thank the Department of Surgery, University of Pittsburgh Medical Center for continued support. LP thanks the American College of Surgeons for support via ACS fellowship # 709532. SV thanks the American Chemical Society-Petroleum Research Fund grant 533–86-ND7 and NSF 1561789 for funding. EC thanks the FONDECYT Grant # 1161098. LP, SV, and ET thank the University of Pittsburgh Center for Medical Innovation for support via CMI grant # F-123–2015. We also thank Joseph Hanke, Teri Horgan and others who obtained the fresh ovine blood used in this study and the Center of Biological Imaging (CBI) of the University of Pittsburgh for allowing the use of SEM.

References

[1]. Michiels C, Endothelial cell functions, J. Cell. Physiol 196 (2003) 430–443. [PubMed: 12891700]

[2]. Lavery KS, Rhodes C, McGraw A, Eppihimer MJ, Anti-thrombotic technologies for medical devices, Adv. Drug Deliv. Rev 112 (2017) 2–11. [PubMed: 27496703]

[3]. Hasebe T, Shimada A, Suzuki T, Matsuoka Y, Saito T, Yohena S, Kamijo A, Shiraga N, Higuchi M, Kimura K, Yoshimura H, Kuribayashi S, Fluorinated diamond-like carbon as antithrombogenic coating for blood-contacting devices, J. Biomed. Mater. Res 76A (2006) 86–94.

[4]. Biran R, Pond D, Heparin coatings for improving blood compatibility of medical devices, Adv. Drug Deliv. Rev 112 (2017) 12–23. [PubMed: 28042080]

[5]. Park K, Shim HS, Dewanjee MK, Eigler NL, In vitro and in vivo studies of PEO-grafted blood-contacting cardiovascular prostheses, J. Biomater. Sci. Polym. Ed 11 (2000) 1121–1134. [PubMed: 11263803]

[6]. Ye SH, Watanabe J, Iwasaki Y, Ishihara K, Antifouling blood purification membrane composed of cellulose acetate and phospholipid polymer, Biomaterials 24 (2003) 4143–4152. [PubMed: 12853244]

[7]. Ye SH, Arazawa DT, Zhu Y, Shankarraman V, Malkin AD, Kimmel JD, Gamble LJ, Ishihara K, Federspiel WJ, Wagner WR, Hollow fiber membrane modification with functional zwitterionic macromolecules for improved throm-boresistance in artificial lungs, Langmuir 31 (2015) 2463–2471. [PubMed: 25669307]

[8]. Desai M, Seifalian AM, Hamilton G, Role of prosthetic conduits in coronary artery bypass grafting, Eur. J. Cardio. Thorac. Surg. 40 (2011) 394–398.

[9]. Devine C, McCollum C, Heparin-bonded Dacron or polytetrafluorethylene for femoropopliteal bypass: five-year results of a prospective randomized multicenter clinical trial, J. Vasc. Surg. 40 (2004) 924–931. [PubMed: 15557906]

[10]. Albers M, Romiti M, Brochado-Neto FC, Pereira CAB, Meta-analysis of alternate autologous veinn bypass grafts to infrapopliteal arteries, J. Vasc. Surg. 42 (2005) 449–455. [PubMed: 16171586]

[11]. Barnes AC, Bieze TWN, Enderby JE, Leyte JC, Dynamics of water in the poly (ethylene oxide) hydration shell: a quasi elastic neutron-scattering study, J. Phys. Chem. 98 (1994) 11527–11532.

[12]. Heyligers JMM, Verhagen HJM, Rotmans JI, Weeterings C, de Groot PG, Moll FL, Lisman T, Heparin immobilization reduces thrombogenicity of small-caliber expanded polytetrafluoroethylene grafts, J. Vasc. Surg. 43 (2006) 587–591. [PubMed: 16520178]

[13]. Genzer J, Groenewold J, Soft matter with hard skin: from skin wrinkles to tem-plating and material characterization, Soft Matter 2 (2006) 310–323.

[14]. Pocivavsek L, Leahy B, Holten-Andersen N, Lin BH, Lee KYC, Cerda E, Geometric tools for complex interfaces: from lung surfactant to the mussel byssus, Soft Matter 5 (2009) 1963–1968.

[15]. Bhushan B, Biomimetics: lessons from nature - an overview, Phil. Trans. Math. Phys. Eng. Sci. 367 (2009) 1445–1486.

[16]. Greensmith JE, Duling BR, Morphology of the constricted arteriolar wall - physiological implications, Am. J. Physiol. 247 (1984) H687–H698. [PubMed: 6496751]

[17]. Walton LA, Bradley RS, Withers PJ, Newton VL, Watson REB, Austin C, Sherratt MJ, Morphological characterisation of unstained and intact tissue microarchitecture by X-ray computed micro- and nano-tomography, Sci. Rep. 5 (2015) 10074. [PubMed: 25975937]

[18]. Pocivavsek L, Pugar J, O'Dea R, Ye S-H, Wagner W, Tzeng E, Velankar S, Cerda E, Topography-driven surface renewal, Nat. Phys. 14 (2018) 948–953.

[19]. Myan FWY, Walker J, Paramor O, The interaction of marine fouling organisms with topography of varied scale and geometry: a review, Biointerphases 8 (2013).

[20]. Graham MV, Cady NC, Nano and microscale topographies for the prevention of bacterial surface fouling, Coatings 4 (2014) 37–59.

[21]. Koh LB, Rodriguez I, Zhou JJ, Platelet adhesion studies on nanostructured poly (lactic-co-glycolic-acid)-carbon nanotube composite, J. Biomed. Mater. Res. 86A (2008) 394–401.

[22]. Mao C, Liang CX, Luo WP, Bao JC, Shen J, Hou XM, Zhao WB, Preparation of lotus-leaf-like polystyrene micro- and nanostructure films and its blood compatibility, J. Mater. Chem. 19 (2009) 9025–9029.

[23]. Chen L, Liu MJ, Bai H, Chen PP, Xia F, Han D, Jiang L, Antiplatelet and thermally responsive poly(N-isopropylacrylamide) surface with nanoscale topography, J. Am. Chem. Soc. 131 (2009) 10467–10472. [PubMed: 19722623]

[24]. Koh LB, Rodriguez I, Venkatraman SS, The effect of topography of polymer surfaces on platelet adhesion, Biomaterials 31 (2010) 1533–1545. [PubMed: 19945746]

[25]. Chen L, Han D, Jiang L, On improving blood compatibility: from bioinspired to synthetic design and fabrication of biointerfacial topography at micro/nano scales, Colloids Surfaces B Biointerfaces 85 (2011) 2–7. [PubMed: 21106352]

[26]. Xu LC, Siedlecki CA, Protein adsorption, platelet adhesion, and bacterial adhesion to polyethylene-glycol-textured polyurethane biomaterial surfaces, J. Biomed. Mater. Res. B Appl. Biomater. 105 (2017) 668–678. [PubMed: 26669615]

[27]. Shivapooja P, Wang QM, Orihuela B, Rittschof D, Lopez GP, Zhao XH, Bioinspired surfaces with dynamic topography for active control of biofouling, Adv. Mat. 25 (2013) 1430–1434.

[28]. Shivapooja P, Wang QM, Szott LM, Orihuela B, Rittschof D, Zhao XH, Lopez GP, Dynamic surface deformation of silicone elastomers for management of marine biofouling: laboratory and field studies using pneumatic actuation, Biofouling 31 (2015) 265–274. [PubMed: 25917206]

[29]. Levering V, Wang QM, Shivapooja P, Zhao XH, Lopez GP, Soft robotic concepts in catheter design: an on-demand fouling-release urinary catheter, Adv. Healthcare Mater. 3 (2014) 1588–1596.

[30]. Gu H, Lee SW, Buffington SL, Henderson JH, Ren DC, On-demand removal of bacterial biofilms via shape memory activation, ACS Appl. Mater. Interfaces 8 (2016) 21140–21144. [PubMed: 27517738]

[31]. Safar ME, Chapter 9: geometry and stiffness of the arterial wall in essential hypertension, in: Safar ME, O'Rourke MF (Eds.), The Arterial System in Hypertension, Springer, Dordrecht, 1993.

[32]. Efimenko K, Wallace WE, Genzer J, Surface modification of Sylgard-184 poly (dimethyl siloxane) networks by ultraviolet and ultraviolet/ozone treatment, J. Colloid Interface Sci. 254 (2002) 306–315. [PubMed: 12702402]

[33]. Ye SH, Hong Y, Sakaguchi H, Shankarraman V, Luketich SK, D'Amore A, Wagner WR, Nonthrombogenic, biodegradable elastomeric polyurethanes with variable sulfobetaine content, ACS Appl. Mater. Interfaces 6 (2014) 22796–22806. [PubMed: 25415875]

[34]. Ye S-H, Johnson CA Jr., Woolley JR, Murata H, Gamble LJ, Ishihara K, Wagner WR, Simple surface modification of a titanium alloy with silanated zwitterionic phosphorylcholine or sulfobetaine modifiers to reduce thrombogenicity, Colloids Surfaces B Biointerfaces 79 (2010) 357–364. [PubMed: 20547042]

[35]. Milleret V, Hefti T, Hall H, Vogel V, Eberli D, Influence of the fiber diameter and surface roughness of electrospun vascular grafts on blood activation, Acta Biomater. 8 (2012) 4349–4356. [PubMed: 22842036]

[36]. Linneweber J, Dohmen PM, Kerzscher U, Affeld K, Nose Y, Konertz W, The effect of surface roughness on activation of the coagulation system and platelet adhesion in rotary blood pumps, Artif. Organs 31 (2007) 345–351. [PubMed: 17470203]

[37]. Zingg W, Neumann AW, Strong AB, Hum OS, Absolom DR, Effect of surface-roughness on platelet-adhesion under static and under flow conditions, Can. J. Surg. 25 (1982) 16–19. [PubMed: 7055757]

[38]. Regar E, van Leeuwen TG, Serruys PW (Eds.), Optical Coherence Tomography in Cardiovascular Research, Informa Healthcare, London, 2007.

[39]. Patel D, Vaananen H, Jirouskova M, Hoffmann T, Bodian C, Coller BS, Dynamics of GPIIb/IIIa-mediated platelet-platelet interactions in platelet adhesion/thrombus formation on collagen in vitro as revealed by videomicroscopy, Blood 101 (2003) 929–936. [PubMed: 12529292]

[40]. Jiang HQ, Khang DY, Song JZ, Sun YG, Huang YG, Rogers JA, Finite de-formation mechanics in buckled thin films on compliant supports, Proc. Natl. Acad. Sci. Unit. States Am. 104 (2007) 15607–15612.

[41]. Begley MR, Hutchinson JW, The Mechanics and Reliability of Films, Multilayers, and Coatings, Cambridge University Press, Cambridge, 2017.

[42]. Cuvelier D, Théry M, Chu Y-S, Dufour S, Thiéry J-P, Bornens M, Nassoy P, Mahadevan L, The universal dynamics of cell spreading, Curr. Biol. 17 (2007) 694–699. [PubMed: 17379524]

[43]. Epstein AK, Hong D, Kim P, Aizenberg J, Biofilm attachment reduction on bioinspired, dynamic, micro-wrinkling surfaces, New J. Phys. 15 (2013).

[44]. Liang C, Hu Y, Wang H, Xia D, Li Q, Zhang J, Yang J, Li B, Li H, Han D, Dong M, Biomimetic cardiovascular stents for in vivo re-endothelialization, Biomaterials 103 (2016) 170–182. [PubMed: 27380443]

[45]. Bettinger CJ, Langer R, Borenstein JT, Engineering substrate topography at the micro- and nanoscale to control cell function, Angew. Chem. Int. Ed. 48 (2009) 5406–5415.

[46]. Teixeira AI, Abrams GA, Bertics PJ, Murphy CJ, Nealey PF, Epithelial contact guidance on well-defined micro- and nanostructured substrates, J. Cell Sci. 116 (2003) 1881–1892. [PubMed: 12692189]

[47]. Nikkhah M, Edalat F, Manoucheri S, Khademhosseini A, Engineering microscale topographies to control the cell-substrate interface, Biomaterials 33 (2012) 5230–5246. [PubMed: 22521491]

[48]. Jansen JA, Von Recum AF, Chapter 2.15: textured and porous materials, in: Ratner BD, Hoffman AS, Schoen FJ, Lemons JE (Eds.), Biomaterials Science: an Introduction to Materials in Medicine, second ed, Elsevier, Amsterdam, 2004.

[49]. Okeyo KO, Miyoshi H, Adachi T, Chapter 10: cell migration in engineered mi-crotextured surfaces, Innovative Approaches to Cell Biomechanics: from Cell Migration to On-chip Manipulation, Springer, Tokyo, 2015.

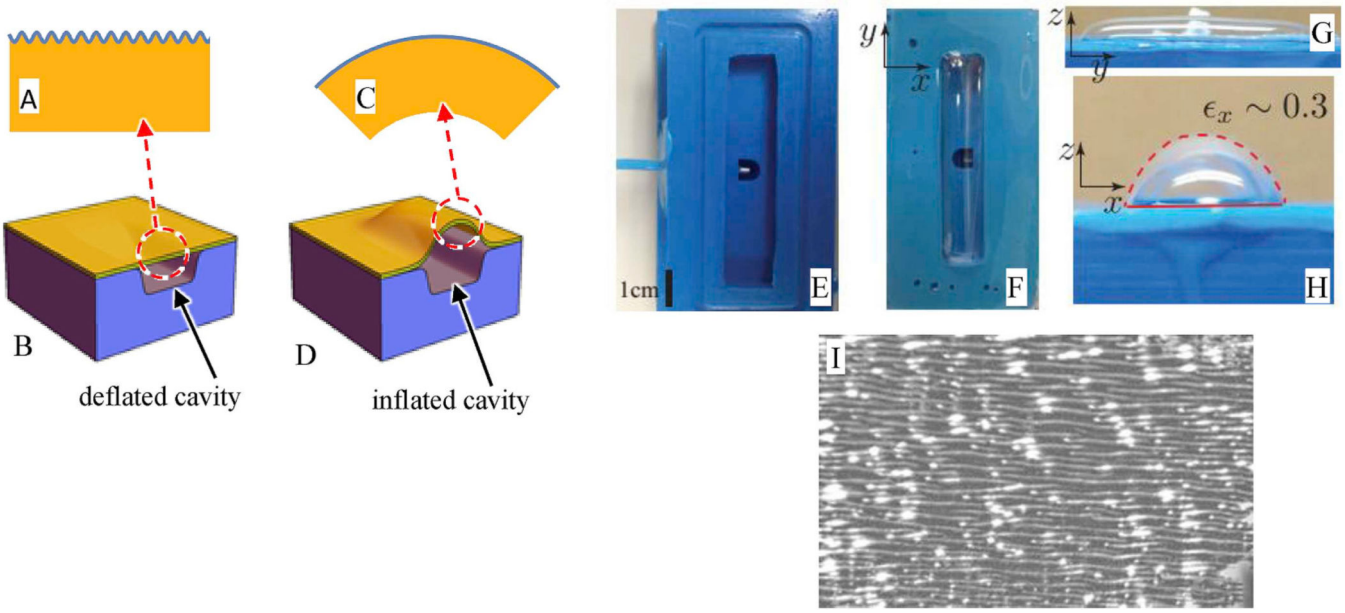

Fig. 1.

A-D: Schematics of the mechanics of wrinkle actuation by inflation. The cavity in the actuator base (lowest blue block) can be inflated or deflated, which induces expansion/contraction of the elastomeric sheet (yellow). The thin film (upper blue line) can then become smooth or wrinkled.E. Top view of the actuator base (the elastomeric sheet is not yet attached). The rectangular cavity in the center can be pressurized via the visible hole. F (top view) and G&H side views of the device while inflated. I: Optical image of the wrinkled surface in a deflated state. The bright white spots are an artifact of the reflection illumination. (For interpretation of the references to colour in this figure legend, the reader is referred to the Web version of this article.)

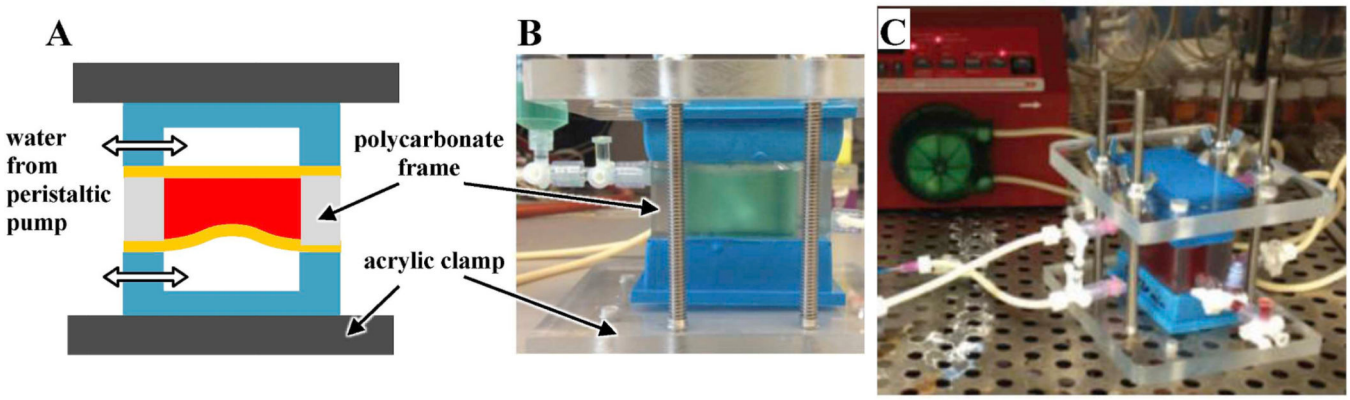

Fig. 2.

A. Schematic of “opposed chamber”. The thick yellow lines represent the PDMS elastomeric sheets, with the test surfaces facing the blood side (red). Note that the two chambers (blue) are actuated out of phase so that one sheet is inflating while the other deflates. The acrylic clamps are held together by long bolts (not shown in A, but visible in B). **B.** The opposed chamber shown when filled with green water for illustration.**C.** Blood experiment in progress with peristaltic pump in the background. (For interpretation of the references to colour in this figure legend, the reader is referred to the Web version of this article.)

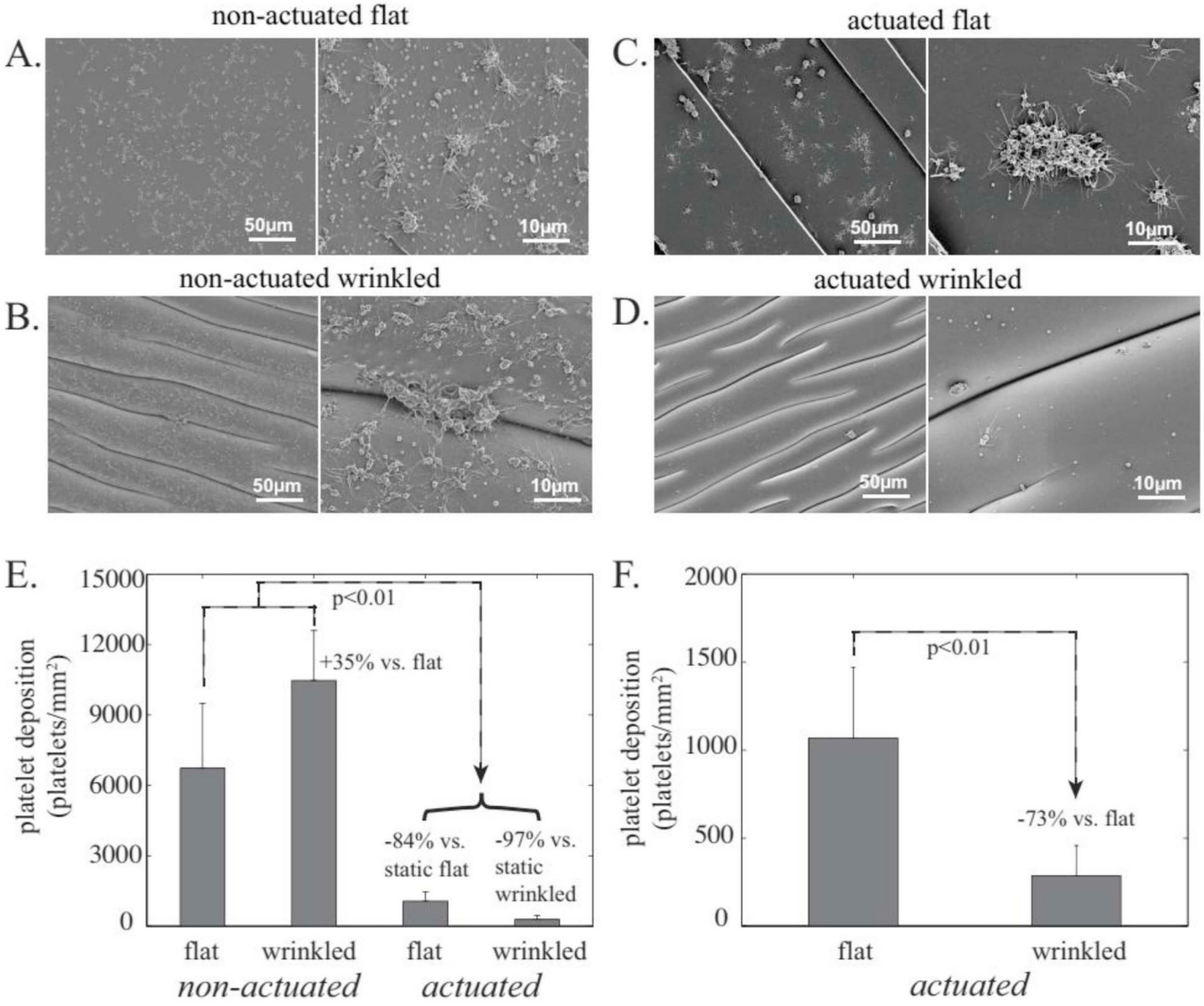

Fig. 3.

A-D: SEM images of the various surfaces tested, each shown at two different magnifications. **E.** Quantitative comparison (using LDH assay) of the four surfaces, and **F.** Comparison of two actuated samples (same data as **E**).

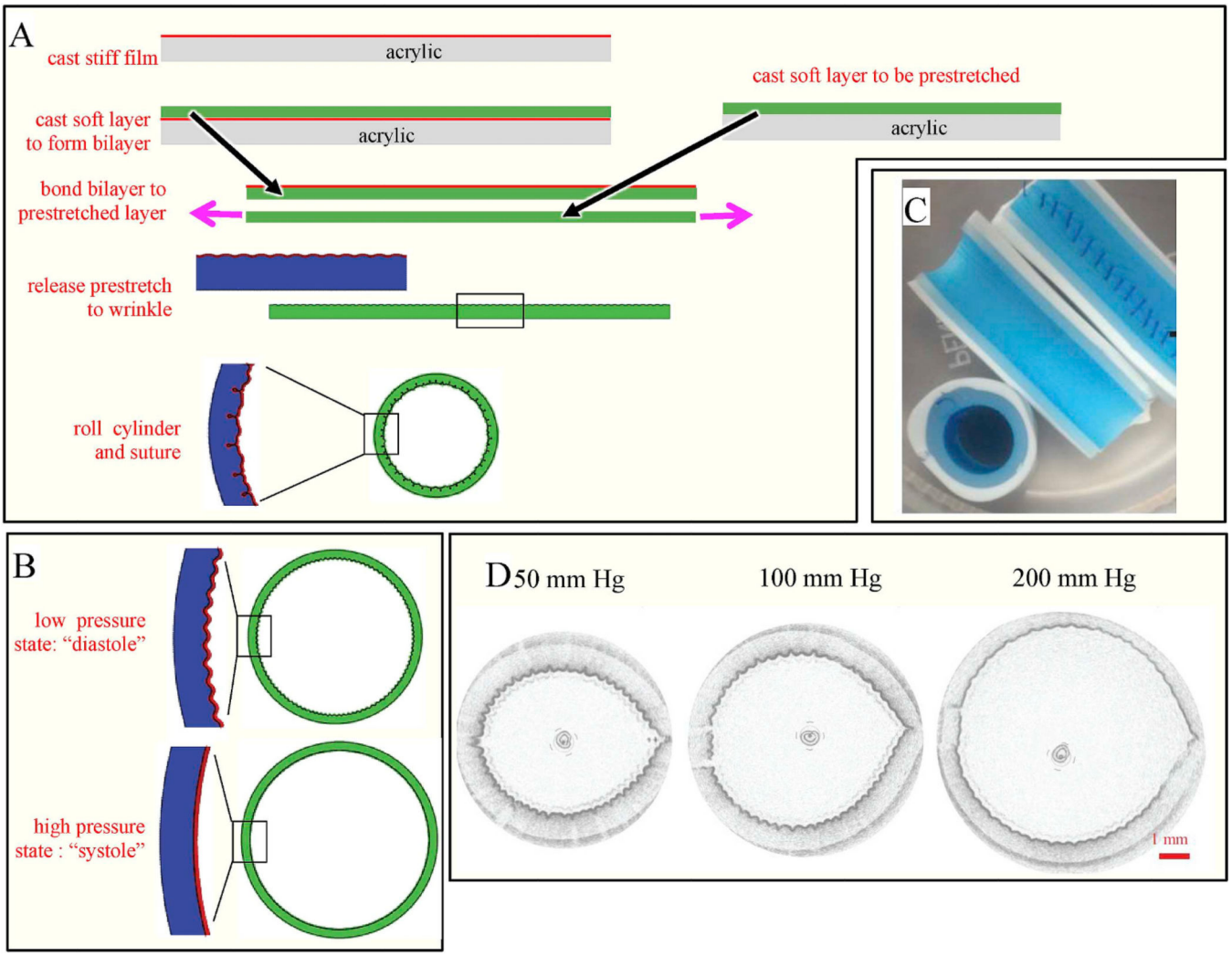

Fig. 4.

A. Schematic of process used for fabricating cylindrical tubes. **B.** Schematic of the cross section of a cylindrical tube that transitions from wrinkled to smooth upon inflation. **C.** Image of the fabricated tube including a view of the sutures. **D.** OCT images of a tube inflated with water to reduce the degree of wrinkling.

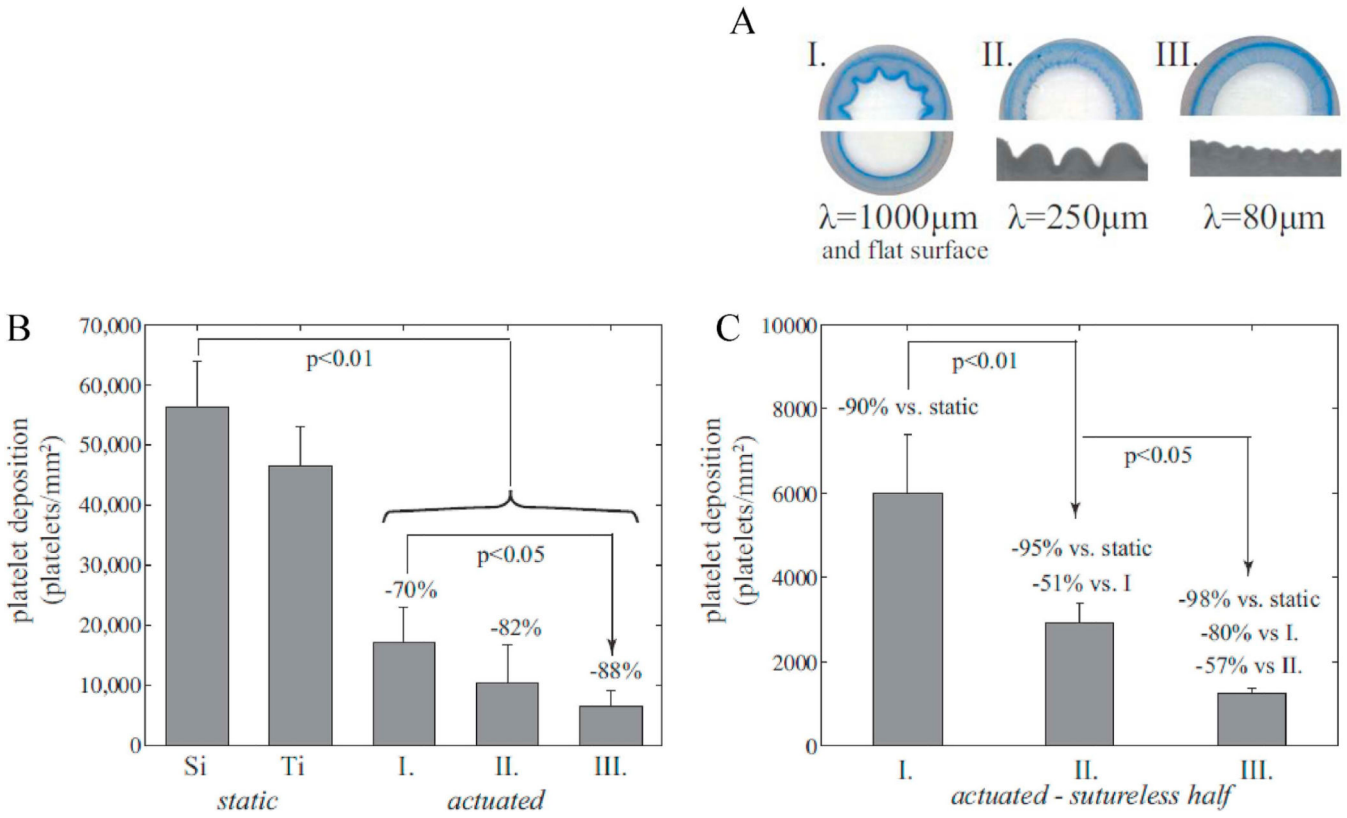

Fig. 5.

A. Cross sections of four test samples (where the flat surface and the 1000 μm wavelength are grouped together in I). B. Platelet deposition as measured from LDH assay comparing the three samples of A against controls static silicone (labeled Si) and $TiAl_6V_4$ (labeled Ti). C. Platelet deposition on the sutureless hemi-cylinder of samples of A.

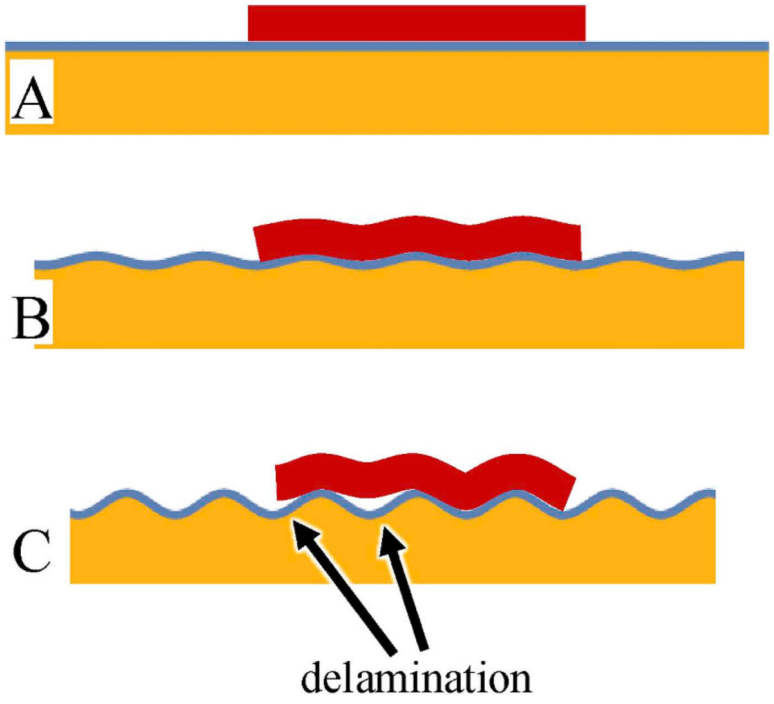

Fig. 6.

Schematic of proposed mechanism (see text). A: a biofoulant patch (dark red) adheres to a flat substrate. The flat substrate itself consists of a thin, stiff film (shown as a thin blue line) bonded to a softer underlayer (orange) B: The surface compresses and hence develop wrinkles. The patch follows the deformation. C: Wrinkle amplitude increases and the patch delaminates. (For interpretation of the references to colour in this figure legend, the reader is referred to the Web version of this article.)